Morphology and crystallography of β precipitate phase in Mg−Gd−Y−Nd−Zr alloy

LI Ting[1], DU Zhi-wei[2], ZHANG Kui[1], LI Xing-gang[1], YUAN Jia-wei[1], LI Yong-jun[1], MA Ming-long[1], SHI Guo-liang[1]

1. State Key Laboratory for Fabrication and Processing of Nonferrous Metals,
Beijing General Research Institute for Nonferrous Metals, Beijing 100088, China;
2. National Analysis and Testing Center for Nonferrous Metals & Electronic Materials,
Beijing General Research Institute for Nonferrous Metals, Beijing 100088, China

Abstract: Morphology and crystal structure of β precipitate phase in Mg−7Gd−5Y−1Nd−0.5Zr (mass fraction, %) alloy were characterized by optical microscopy, scanning electron microscopy and transmission electron microscopy. Compositions were determined for β phase using thin foil energy dispersive spectroscopy. Precipitation at 400 °C involves formation of $(1\bar{1}00)_\alpha$ platelet and block-shaped β phase. The orientation relationship is $(\bar{2}11)_\beta //(01\bar{1}0)_\alpha$ and $[0\bar{1}1]_\beta //[0001]_\alpha$ between β precipitate phase and α-Mg matrix with habit planes parallel to $(1\bar{1}00)_\alpha$, and a composition of $Mg_5(Y_{0.4}Gd_{0.4}Nd_{0.2})$ is suggested for the β phase in Mg−7Gd−5Y−1Nd−0.5Zr alloy.

Key words: Mg−Gd−Y−Nd−Zr alloy; precipitation phase; microstructure; composition; orientation relationship; habit plane

1 Introduction

Magnesium−rare earth alloys containing yttrium or heavy rare earth elements offer attractive properties for the aerospace and automotive industries [1−3]. It has been reported that the recently developed Mg−Gd−Y−Nd−Zr alloy, exhibits high specific strength at both room and elevated temperatures [4,5]. The strength of Mg−Gd−Y−Nd−Zr alloy is achieved essentially via precipitation strengthening [6]. However, the precipitation behavior and composition of various precipitation phases in Mg−Gd−Y−Nd−Zr alloy is not fully understood.

It was reported that the ternary Mg−Y−Nd, Mg−Gd−Nd alloys [7−12] exhibit a four-stage precipitation sequence during aging heat treatment, α-Mg(S.S.S.S) $\rightarrow \beta''$(CBCO) $\rightarrow \beta'$(CBCO) $\rightarrow \beta_1$(FCC) $\rightarrow \beta$(FCC). The metastable phase β'' has a DO19 crystal structure (hexagon, a=0.642 nm, b=0.521 nm), the orientation relationship between β'' and matrix is in the forms of $(2\bar{1}\bar{1}0)_{\beta''} //(2\bar{1}\bar{1}0)_\alpha$ and $[0001]_{\beta''} //[0001]_\alpha$. The intermediate phase β' has a base-centered orthorhombic structure (CBCO, a=0.640 nm, b=2.223

nm, c=0.521 nm), and the orientation relationship is $(100)_{\beta'} //(1\bar{2}10)_\alpha$ and $[001]_{\beta'} //[0001]_\alpha$. The β_1 phase has a face-centered cubic structure (FCC, space group $Fm\bar{3}m$, a=0.74 nm), and the orientation relationship is $(\bar{1}12)_{\beta_1} //(1\bar{1}00)_\alpha$ and $[001]_{\beta_1} //[0001]_\alpha$. The equilibrium phase β has a face-centered cubic structure (FCC, space group $F\bar{4}3m$, a=2.23 nm). The β phase is transformed in situ from β_1, thus the orientation relationship is sustained. However, the three-stage precipitation sequence has been reported on binary alloys Mg−Gd and Mg−Y, without the formation of β_1 [13,14].

The present work aims at clarifying the morphology, structure and composition of β phase in Mg−Gd−Y−Nd−Zr alloy formed during heat treatment at 400 °C.

2 Experimental

An alloy ingot with nominal composition of Mg−6.85Gd−4.52Y−1.12Nd−0.55Zr (mass fraction, %) was fabricated in a medium-frequency induction furnace under RJ-2 flux-refining. To prevent overheating of as-cast eutectic structure, a two-step solution treatment (440 °C for 6 h and 535 °C for 16 h) was carried out for the samples cut form the ingot. The next steps of heat

treatment included: 1) water quenching at room temperature and aging at 400 °C for 6 h; and 2) cooling down after solution heat treatment from 535 °C to 400 °C and holding for 6 h.

In order to determine the microstructure, optical microscopy (OM), scanning electron microscopy (SEM) and transmission electron microscopy (TEM) were used. Meanwhile, thin foil energy dispersive spectroscopy (EDS) was used for phase composition analysis. To reveal the microstructure, the polished samples prepared for OM and SEM were etched in a 4% solution of HNO_3 in C_2H_5OH for about 60 s. Discs with 3 mm in diameter were punched from the heat treated samples, ground to a thickness of 0.06 mm, and twin-jet electro polished in a solution of 15 mL perchloric acid and 285 mL ethanol, at −30 °C and 0.01 A. Microstructure examination was performed in a JEM−2000 operating at 160 kV. Quantitative energy dispersive spectroscopy was carried out to determine the composition of the precipitate phases.

3 Results and discussion

3.1 Microstructure of as-cast alloy

Figure 1 and Table 1 show the typical SEM image of as-cast Mg−7Gd−5Y−1Nd−0.5Zr alloy and the corresponding EDS results. Non-equilibrium solidification conditions cause the heavy segregation of alloying elements at the grain boundaries and interdendrical spaces, thus the dendritic structure of as-cast alloy is typical. The microstructure consists of α-Mg matrix, block-shaped compounds (indicated by A) rich in Y and Gd, and eutectic phase (indicated by B) designated as $Mg_{24}Y_5$, $Mg_{5.05}Gd$, $Mg_{41}Nd_5$ and Mg_3Gd
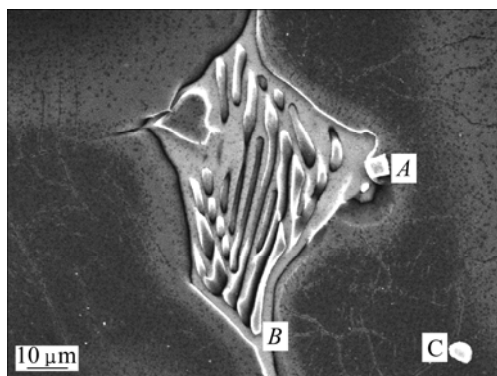

Fig. 1 SEM micrograph of as-cast EW75 alloy

Table 1 EDS results of as-cast EW75 alloy in Fig. 1

Position	w(Mg)/%	w(Y)/%	w(Gd)/%	w(Nd)/%	w(Zr)/%
A	−	56.38	43.62	−	−
B	5071	7.85	28.78	12.67	−
C	3.31	−	−	−	96.69

[15]. In addition, Zr particles (indicated by C) distribute in the α-Mg matrix to make the grain refine.

3.2 Microstructure of solution-treated alloys

To prevent overheating of as-cast eutectic structure, a two-step solution treatment (440 °C for 6 h and 535 °C for 16 h) was carried out. The microstructure obtained after solution heat treatment is shown in Fig. 2. It could be seen that the white net-work eutectic structures in the as-cast alloys have been completely dissolved, and a two-step solution heat treatment of Mg−7Gd−5Y−1Nd−0.5Zr alloy causes a total dissolution of the eutectic structures throughout the matrix. However, the coarse block-shaped compounds rich in Y and Gd still exist. The corresponding EDS results in Table 2 show that the compounds did not change during the heat treatment. Thus, the solution treated microstructure consists of Y−Gd phase and Zr particles, as shown in Fig. 2.
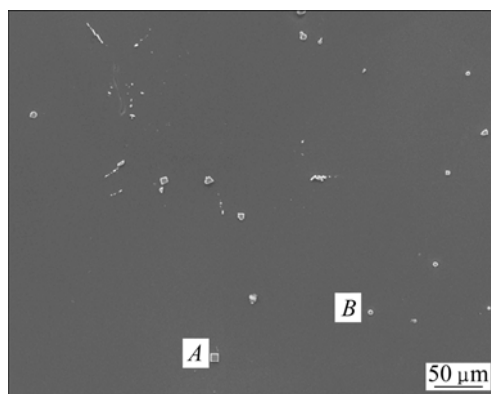

Fig. 2 SEM micrograph of solution-treated EW75 alloy

**Table 2** EDS results of solution-treated EW75 alloy in Fig. 2

Position	w(Mg)/%	w(Y)/%	w(Gd)/%	w(Nd)/%	w(Zr)/%
A	1.35	64.21	31.81	2.64	−
B	7.12	−	−	−	92.88

3.3 Microstructure of precipitate phases

The OM images of precipitates in Mg−7Gd−5Y−1Nd−0.5Zr alloy after 400 °C heat treatment are shown in Fig. 3. Both cases of 1) water quenching at room temperature and aging at 400 °C for 6 h and 2) cooling down after solution heat treatment from 535 °C to 400 °C and holding for 6 h of precipitation formation are presented schematically in Fig. 4. The microstructures after cooling from 535 °C to 400 °C and holding for 10 min for supersaturated samples are shown in Fig. 3(a). Unlike the $Mg_{17}Al_{12}$ precipitates that are lamellar in Mg−Al alloys [16], the precipitate phase in Mg−7Gd−5Y−1Nd−0.5Zr alloy distribute in different orientations, which indicates the precipitates may have
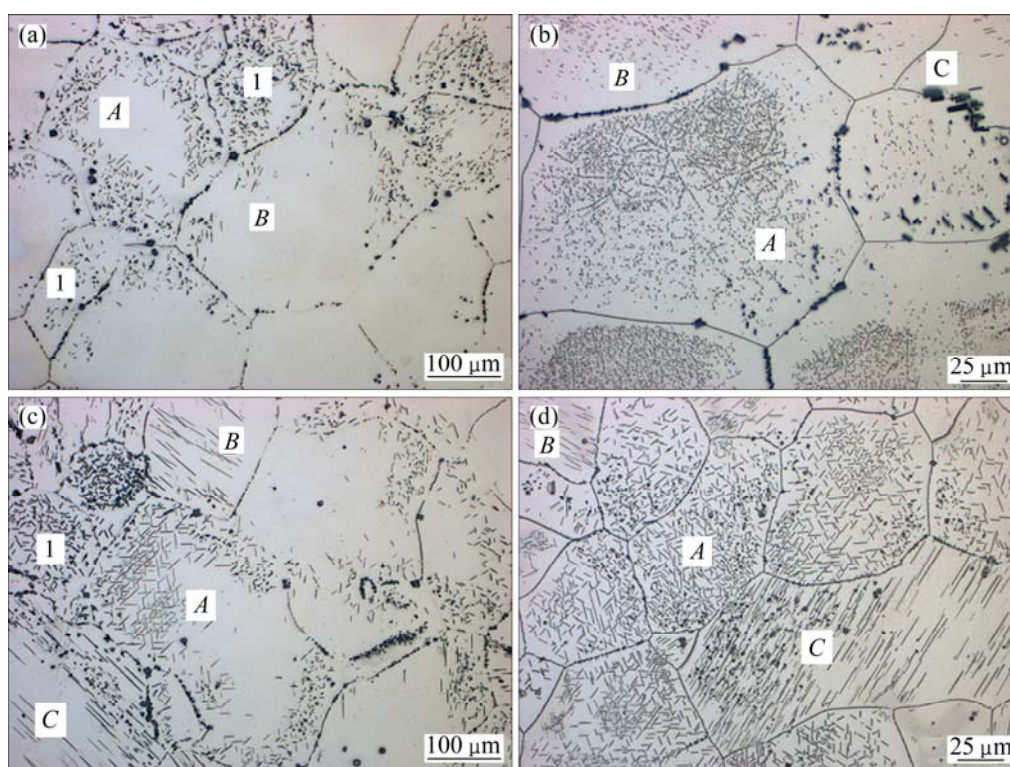
Fig. 3 OM image showing precipitates of EW75 alloy after heat treatment: (a) Cooling from 535 °C to 400 °C and holding for 10 min; (b) Aging at 400 °C for 10 min; (c) Cooling from 535 °C to 400 °C and holding for 6 h; (d) Aging at 400 °C for 6 h
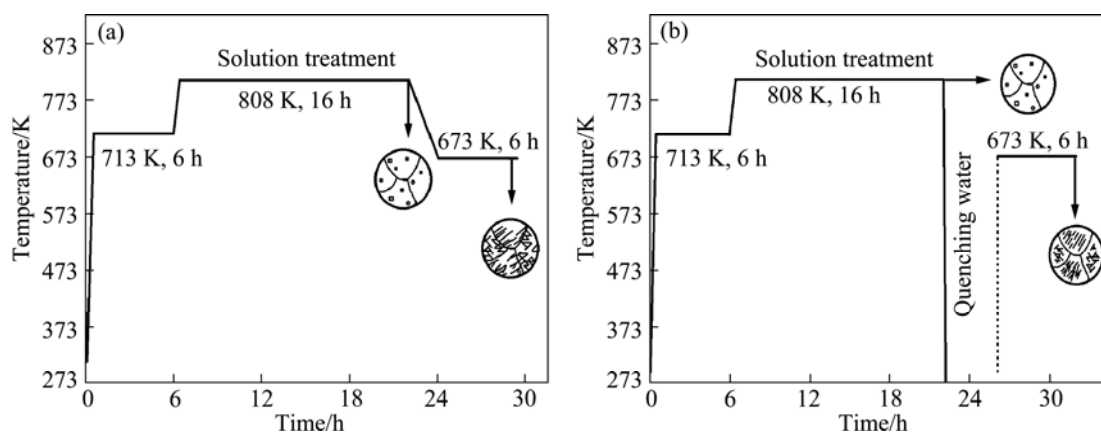
Fig. 4 Schemes of precipitation in EW75 alloy depending on heat treatment: (a) Cooling from solution treatment temperature (without quenching) and holding at 400 °C; (b) Aging of supersaturated (and quenching in water) solid solution at 400 °C

different orientation relationships with matrix or different variants of the same orientation relationships. The precipitate phase formed inhomogenously throughout the α-Mg matrix. The plate-like precipitates distribute dispersedly in some grains (indicated by 1 in Fig. 3), but in most grains, precipitates appear at the grain boundaries and the regions nearby. The arrangement of precipitates can be in either triangle (indicated by *A*) or as a herringbone (indicated by *B*), or along a specific direction (indicated by *C*). After holding at 400 °C for 6 h, precipitates have grown up along the length direction

of the plates, and the arrangement of precipitates is identical, as shown in Fig. 3(c).

Figure 3(b) shows the OM images of Mg−7Gd−5Y−1Nd−0.5Zr alloy after aging at 400 °C for 10 min. The microstructure is characterized by the presence of a large amount of dispersive precipitate shown in Fig. 3(b). The morphology of the precipitates in Fig. 3(b) is exactly the same as that in Fig. 3(a), suggesting that the precipitate phase formed during 400 °C is not affected by different heat treatment ways. However, the size and distribution of precipitates are different. Small plate-like

precipitates inside the grains are observed in most grains and these precipitates can rarely been observed at the grain boundaries, which is different from the microstructure shown in Fig. 3(a).

The different cases of precipitation formation are presented schematically in Fig. 4. A two-step solution heat treatment was carried out to prevent overheating of eutectic structures in as-cast alloys. The solution-treated microstructure consists of Y−Gd phase and Zr particles. The precipitation structures formed in both cases 1) and 2) are shown in Figs. 4(a) and (b), respectively. The precipitates formed immediately at the early stage of heat treatment, the arrangement of precipitates is identical in both cases, which can be either in triangle or as a herringbone, or along a specific direction. However, the precipitates distribution is different. In Fig. 4(b), the plate-like precipitates form inside the grains, but precipitates appear at the grain boundaries and the regions nearby in Fig. 4(a). The precipitation behavior is not exactly the same because the subcooling temperature for precipitation of aged samples is lower. The driving force of phase transformation is stronger for the aged samples, thus precipitates nucleate uniformly inside the grains. On the other hand, the driving force is not so strong for directly cooled samples that precipitate phases nucleate at the grain boundaries and regions nearby with

disorganized structures.

3.4 Morphology and crystal structure of precipitate phases

A bright field micrograph of typical microstructure in samples aged at 400 °C for 6 h is shown in Fig. 5, with the electron beam parallel to $[0001]_\alpha$. The microstructures contain numerous platelets with length around 5 μm. These plates distribute homogenously and lie in three $(1\bar{1}00)_\alpha$ planes. The triangle arrangements of precipitates can be seen in Fig. 5(a), the angle between two precipitate plates is approximately 60°, which indicates that the different orientation of β is due to the variant of the same relationship. The three variants are identifiable in Fig. 5(a) and the forms of the three variants of the $(1\bar{1}00)_\alpha$ plates are represented schematically in Fig. 5(b). It can be seen that the β phase forms as plates with habit plane parallel to $(1\bar{1}00)$ and habit direction parallel to $[11\bar{2}0]$. In addition, some precipitates with blocky shape never mentioned before by others (indicated by A in Fig. 5) have been discovered. However, it is difficult to obtain electron diffraction patterns from individual phases to identify their crystal structures.

Figure 6 shows the typical microstructures of plate-shaped phases in samples aged at 400 °C for 6 h,
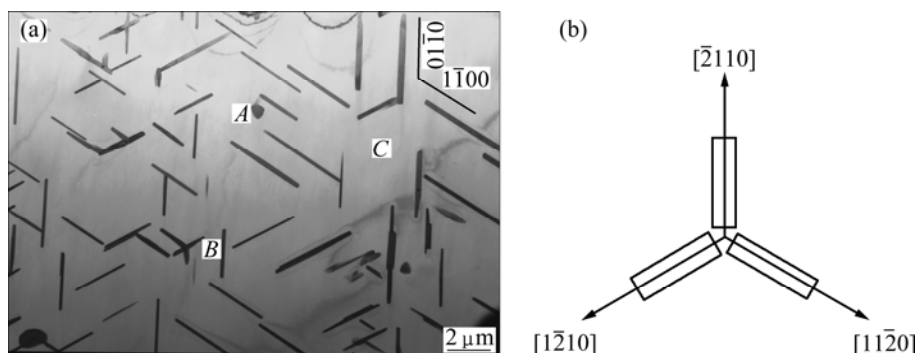
Fig. 5 $[0001]_\alpha$ zone axis bright field image recorded from sample aged at 400 °C for 6 h (a) and corresponding schematic representation of three variants distinguishable in $[0001]_\alpha$ direction (b)
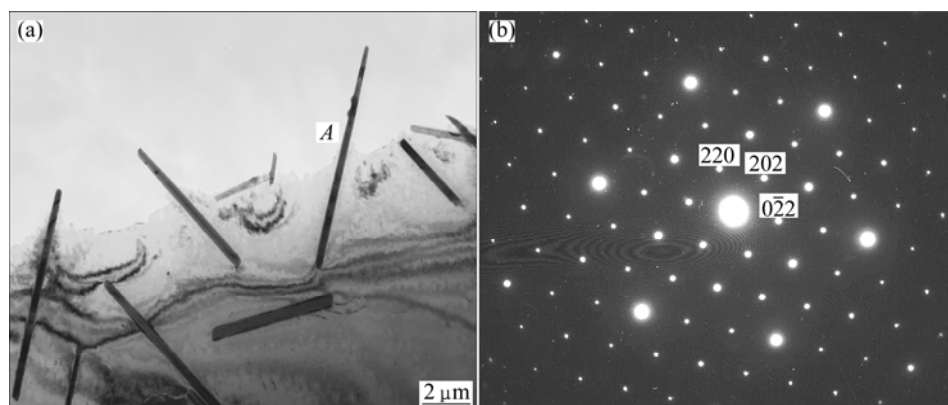
Fig. 6 TEM image showing β precipitates with electron beam parallel to $[11\bar{2}3]$ (a) and corresponding electron diffraction pattern recorded from β phase (b)

with the electron beam parallel to the $[11\bar{2}3]$ direction. The corresponding SEAD pattern of precipitate (indicated by A) is shown in Fig. 6(b). It can be well indexed according to the equilibrium phase β (FCC, a=2.22 nm) that the zone axis of β precipitate is $[\bar{1}11]$.

To determine the orientation relationship between β phase and matrix, the typical electron diffraction pattern recorded along the $[0001]\alpha$ zone axis is shown in Fig. 7. The orientation relationship implied by superimposed precipitate and matrix pattern is $(\bar{2}11)_\beta$ $//(01\bar{1}0)_\alpha$ and $[0\bar{1}1]_\beta$ $//[0001]_\alpha$, which is identical with the orientation relationships discovered in Mg−Gd alloys, Mg−Y−Nd alloys and so on.
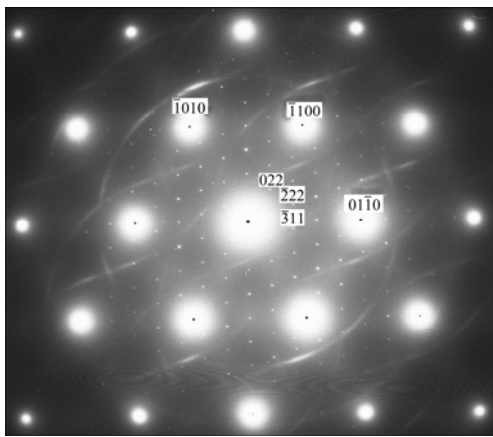

Fig. 7 Electron diffraction pattern recorded from β phase parallel to $[0001]_\alpha$ zone axis

3.5 Composition of β phase

Compositions were investigated for both plate-shaped β phases and block-shaped phases. After examining 30 precipitates, the EDS results of both precipitate phases and matrix (indicated by A, B and C respectively as shown in Fig. 5) are shown in Table 3. Analysis of the matrix is clustered around 99% Mg (mole fraction). The composition of plate-shaped β phase is nearly identical with the block-shaped phase, indicating that block shape is another morphology of β phase.

Table 3 EDS results of points shown in Fig. 5

Position	x(Mg)/%	x(Y)/%	x(Gd)/%	x(Nd)/%	x(Zr)/%
A	83.67	7.54	6.03	2	−
B	86.24	6.90	5.04	1.82	−
C	98.80	0.56	0.44	0.12	−

Analysis of the plate-shaped β phase is clustered around 83% Mg (mole fraction), suggesting a precipitation composition close to Mg$_5$RE [17]. The Nd concentration in phase A is significantly lower than that of Y or Gd, the Y to Gd mole ratio is near 1:1 and Nd to (Y,Gd) mole ratio is 1:2. Hence, a composition of

Mg$_5$(Y$_{0.4}$Gd$_{0.4}$Nd$_{0.2}$) is suggested for the β phase in Mg−7Gd−5Y−1Nd−0.5Zr alloy.

4 Conclusions

1) Compared with the sample directly cooling from 535 °C to 400 °C, the driving force of precipitate phase transformation is stronger for aged sample, thus precipitates nucleate uniformly inside the grains.

2) The β phase (FCC, a=2.22 nm) forms during heat treatment at 400 °C with habit plane parallel to $(1\bar{1}00)$ and habit direction parallel to $[11\bar{2}0]$. The orientation relationships of $(\bar{2}11)_\beta$ $//(01\bar{1}0)_\alpha$ and $[0\bar{1}1]_\beta$ $//[0001]_\alpha$ between β and matrix have been found in Mg−7Gd−5Y−1Nd−0.5Zr alloy. Besides the $(1\bar{1}00)_\alpha$ plates (viewed from $[0001]_\alpha$ direction), another block-shaped morphology of β phase never mentioned before has been discovered.

3) Quantitative EDS analysis has been successfully carried out on the precipitate phases, suggesting that plate-shaped and block-shaped phases can be both identified as β, and a composition of Mg$_5$(Y$_{0.4}$Gd$_{0.4}$Nd$_{0.2}$) is suggested for the β phase in Mg−7Gd−5Y−1Nd−0.5Zr alloy.

References

[1] LORIMER G W, APPS P J, KARIMZADEH H, NIE J F. Improving the performance of Mg-rare alloys by the use of Gd or Dy additions [J]. Materials Science Forum, 2003, 419: 279−284.

[2] CHANG Jian-wei, GUO Xing-wu, PENG Li-ming, DING Wen-jiang, PENG Ying-hong. Characterization of anodic coating formed on Mg−3Nd−0.2Zn−0.4Zr Mg alloy in alkaline electrolyte [J]. Transactions of Nonferrous Metals Society of China, 2008, 18: s318−s322.

[3] SMOLA B, STULIKOVA I, VONBUCH F, MORDLIKE B L. Structure aspects of high performance Mg alloys design [J]. Material Science and Engineering A, 2002, 324: 113−117.

[4] LI Yong-jun. Study on the preparation, microstructures and mechanical properties of Mg−Y−RE−Zr alloys [D]. Beijing: General Research Institute for Nonferrous Metals, 2009. (in Chinese)

[5] LI Yong-jun, ZHANG Kui, LI Xing-gang, MA Ming-long, WANG Hai-zhen, HE Lan-qiang. Influence of extrusion on microstructures and mechanical properties of Mg−5.0Y−7.0Gd−1.3Nd−0.5Zr magnesium alloy [J]. The Chinese Journal of Nonferrous Metals, 2010, 20(9): 1692−1697. (in Chinese)

[6] LIU Zheng, ZHANG Kui, ZENG Xiao-qin. The basic theory and application of magnesium alloys [M]. Beijing: China Machine Press, 2002. (in Chinese)

[7] HONMA T, OHKUBO T, HONO K, KAMADO S. Chemistry of nanoscale precipitates in Mg−2.1Gd−0.6Y−0.2Zr (at.%) alloy investigated by the atom probe technique [J]. Material Science and Engineering A, 2005, 395: 301−306.

[8] NIE J F, MUDDLE B C. Characterisation of strengthening precipitate phases in a Mg−Y−Nd alloy [J]. Acta Materialia, 2000, 48: 1691−1703.

[9] HE S M, ZENG X Q, PENG L M, GAO X, NIE J F. Precipitation in a Mg−10Gd−3Y−0.4Zr (wt.%) alloy during isothermal ageing at 250 °C [J]. Journal of Alloys and Compounds, 2006, 421: 309−313.

[10] NIE J F, MUDELE B C. Precipitation in a Mg−10Gd−3Y−0.4Zr (wt.%) alloy during isothermal ageing at 250 °C [J]. Script Materialia, 1999, 40: 1089−1094.

[11] XIN R L, LI L, ZENG K, SONG B, LIU Q. Structural examination of aging precipitation in a Mg−Y−Nd alloy at different temperatures [J]. Materials Characterization, 2011, 62: 535−539.

[12] PENG Q M, DONG H W, WANG L D, WU Y M, WANG L M. Aging behavior and mechanical properties of Mg−Gd−Ho alloys [J]. Materials Characterization, 2008, 59: 983−986.

[13] VOSTRY P, SMOLA B, STULIKOVA I, VONBUNCH F, MORDLIKE B L. Microstructure evolution in isochronally heat treated Mg−Gd alloys [J]. Physica Status Solidi A, 2002, 175: 491−500.

[14] SOCJUSZ-PODOSEK M, LITYNSKA L. Effect of yttrium on structure and mechanical properties of Mg alloys [J]. Materials Chemistry and Physics, 2003, 80: 472−475.

[15] MA Ming-long, ZHANG Kui, LI Xing-gang, LI Yong-jun, ZHANG Kang. Hot deformation behavior of rare earth magnesium alloy without pre-homogenization treatment [J]. Transactions of Nonferrous Metals Society of China, 2008, 18: 131−139.

[16] BRASZCZYNSKA-MALIK K N. Discontinuous and continuous precipitation in magnesium-aluminium type alloys [J]. Journal of Alloys and Compounds, 2009, 477: 870−876.

[17] APPS P J, KARINZADEH H, KING J F, LORIMER G W. Phase compositions in magnesium-rare earth alloys containing yttrium, gadolinium or dysprosium [J]. Script Materialia, 2003, 48: 475−481.

Mg−Gd−Y−Nd−Zr 合金中 β 相的形貌和晶体学特征

李 婷[1]，杜志伟[2]，张 奎[1]，李兴刚[1]，袁家伟[1]，李永军[1]，马鸣龙[1]，石国梁[1]

1. 北京有色金属研究总院 有色金属材料制备加工国家重点实验室，北京 100088；
2. 北京有色金属研究总院 有色金属及电子材料分析测试中心，北京 100088

摘 要：通过 OM、SEM、TEM 及 EDS 分析，研究 Mg−Gd−Y−Nd−Zr 镁合金中 β 相的形貌、成分和晶体学特征，分析连续冷却与等温时效两种方式对 β 相析出行为的影响规律。结果表明，合金在 400 °C 过时效阶段的沉淀相为 $(1\bar{1}00)_\alpha$ 面上的板状和块状 β 相。β 相以 $(1\bar{1}00)_\alpha$ 为惯习面，与基体的取向关系为 $(\bar{2}11)_\beta$ // $(01\bar{1}0)_\alpha$，$[0\bar{1}1]_\beta$ // $[0001]_\alpha$。根据 EDS 统计分析确定 β 相的成分为 $Mg_5(Y_{0.4}Gd_{0.4}Nd_{0.2})$，与 Mg_5Gd 同型。在连续冷却方式中，相变驱动力较小，晶界等缺陷处结构紊乱，易于松弛、应变，因而优先在晶界附近形核。

关键词：Mg−Gd−Y−Nd−Zr 合金；析出相；微观组织；成分；位相关系；惯习面

(Edited by YANG Hua)